Biologics: Targets and Therapy Dovepress

Open Access Full Text Article ORIGINAL RESEARCH

ACE Loss Drives Renal Cell Carcinoma Growth and Invasion by Modulating AKT-FOXO1

Lei Yin[1–3,*], Lixin Mao[4,*], Rui Yin[5,*], Chengxun Lv[1,*], Xiaokai Shi[4], Chuang Yue[4], Yin Chen[4], Chao Lu[4], Zonglin Wu[1], Kai Xu[4], Wei Cao[4]

[1]Department of Urology, Shidong Hospital, Yangpu District, Shidong Hospital Affiliated to University of Shanghai for Science and Technology, Shanghai, 200438, People's Republic of China; [2]Department of Urology, Ruijin Hospital, Shanghai Jiao Tong University School of Medicine, Shanghai, 200025, People's Republic of China; [3]Department of Urology, Shanghai Ninth People's Hospital, Shanghai Jiao Tong University School of Medicine, Shanghai, 201999, People's Republic of China; [4]Department of Urology, The Affiliated Changzhou Second People's Hospital of Nanjing Medical University, Changzhou, 213000, People's Republic of China; [5]Center for Reproductive Medicine, Shandong Provincial Hospital Affiliated to Shandong University, Jinan, 250012, People's Republic of China

*These authors contributed equally to this work

Correspondence: Kai Xu; Wei Cao, Email jssqxk@126.com; weicao_czey@163.com

Purpose: Emerging literature links the role of the renin-angiotensin-aldosterone system (RAAS) to the progression of cancers. However, the function of RAAS has not been verified in Clear-cell renal cell carcinoma (ccRCC).

Methods: ACE expression in ccRCC tissues was determined using RT-PCR, Western blot, and immunohistochemistry staining. The clinical significance of ACE was evaluated through Cox regression analysis. To assess the impact of ACE expression on ccRCC cell growth, metastasis, and glucose activity, CCK-8 assays, transwell assays, Seahorse detection, and xenograft models were utilized. The mechanisms of ACE and its upstream and downstream regulatory factors were investigated using RNA-seq, chromatin immunoprecipitation (ChIP), and luciferase reporter assays.

Results: RAAS-related gene Angiotensin-Converting Enzyme (ACE) was significantly under expressed in ccRCC cells and tissues. High ACE expression was positively associated with a favorable prognosis in ccRCC patients. Functional studies showed that ACE overexpression suppressed ccRCC cell line OS-RC-2 and A498 growth, metastasis, and glycolysis activities, while its knockdown had the opposite effect. Mechanistically, ACE inhibited ccRCC progression and epithelial-mesenchymal transition (EMT) by disrupting the AKT-FOXO1 signaling pathway. Furthermore, we provide evidence that ACE could enhance everolimus (approved agent for ccRCC) antitumor effect and ACE expression is transcriptionally regulated by ZBTB26.

Conclusion: Our findings investigated the roles and mechanisms of ACE in ccRCC. ACE inhibits the growth and metastasis of ccRCC cells in vitro and in vivo by promoting FOXO1 expression, which is the downstream target of PI3K-AKT pathway. Thus, this research suggests that ACE may be a promising target for new therapeutic strategy in ccRCC.

Keywords: ACE, AKT, FOXO1, clear-cell renal cell carcinoma, everolimus

Introduction

Kidney cancer is one of the most common malignancies worldwide. Clear-cell renal cell carcinoma (ccRCC) is the most common pathological subtype of RCC and often presents an aggressive phenotype.[1] Radical surgery is the mainstay of treatment for early ccRCC at present. However, treatment for patients with advanced ccRCC is difficult and ineffective, and the mortality rate is thus high.[2] Unfortunately, ccRCC patients, especially those with ccRCC, are relatively insensitive to chemotherapy and radiotherapy.[3] Thus, an in-depth study of the molecular mechanisms underlying ccRCC development is a top priority for therapeutic intervention.

Recent studies have shown that increased activity of RAAS is a major risk factor influencing genetic changes and various diseases [4,5]. Indeed, the relationship between RAAS and cancer has recently been highlighted.[6] Notably, different components of RAAS can have distinct roles in carcinogenesis. For example, overexpression of AGTR1 is associated with more aggressive tumor features and worse outcomes in glioblastoma, breast cancer, and cholangiocarcinoma [7–9].

Received: 22 August 2024
Accepted: 12 December 2024
Published: 19 December 2024

© 2024 Yin et al. This work is published and licensed by Dove Medical Press Limited. The full terms of this license are available at https://www.dovepress.com/terms.php and incorporate the Creative Commons Attribution – Non Commercial (unported, v3.0) License (http://creativecommons.org/licenses/by-nc/3.0/). By accessing the work you hereby accept the Terms. Non-commercial uses of the work are permitted without any further permission from Dove Medical Press Limited, provided the work is properly attributed. For permission for commercial use of this work, please see paragraphs 4.2 and 5 of our Terms (https://www.dovepress.com/terms.php).

Graphical Abstract

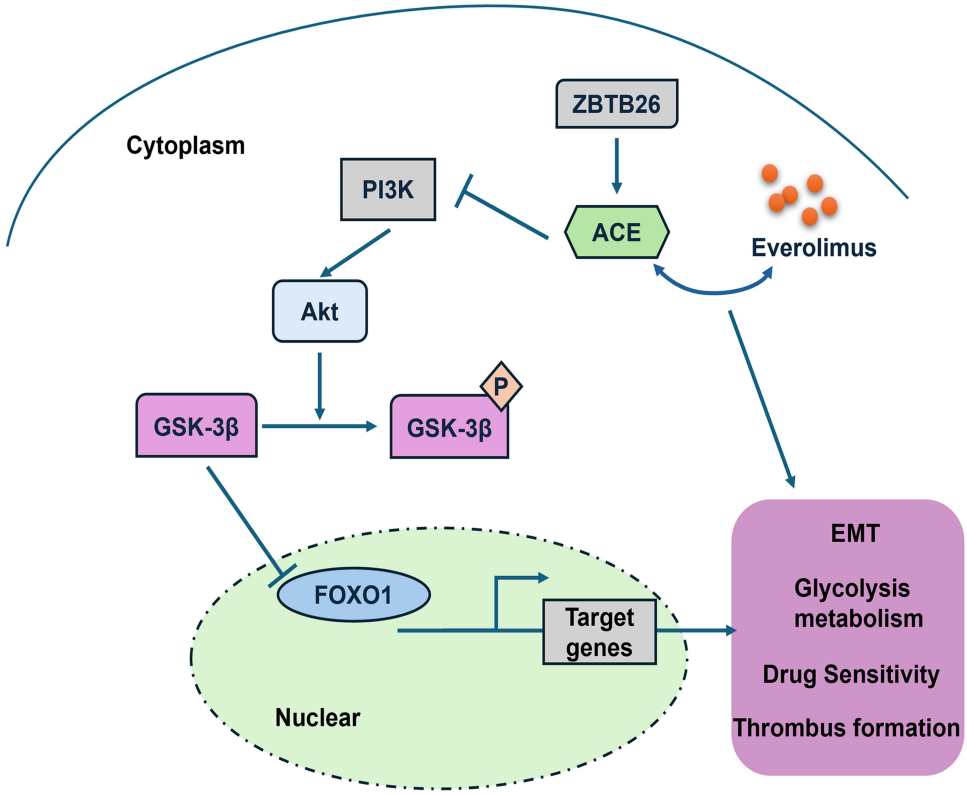

Conversely, AGTR1 inhibits the progression of lung adenocarcinoma.[10] Similarly, ACE2, another peptidase within the RAAS, has been found to prevent tumor growth in gallbladder cancer and hepatocellular carcinoma but facilitates resistance to cisplatin in ovarian carcinoma [11–13]. However, the specific mechanisms of RAAS in ccRCC remain unclear.

In this study, we performed integrative multi-omics analysis and uncovered that ACE, a component of RAAS, is downregulated in ccRCC tumors. High ACE expression predicted better survival in ccRCC patients. Further investigation demonstrated that ACE not only hinders ccRCC cell proliferation, metastasis, and glycolysis activities by inhibiting the AKT-FOXO1 pathway, but also synergized with the therapeutic reagent everolimus. Furthermore, we show that ACE expression is directly regulated transcriptionally by ZBTB26. Our findings indicate that ACE may serve as a valuable biomarker and therapeutic target for ccRCC.

Materials and Methods

Dataset Collection and Processing

To explore the expression levels of RAAS components, we utilized the CPTAC database, which includes protein sequencing data of 118 ccRCC tissues and 84 benign renal tissues. The ccRCC dataset (GSE53757) and ZBTB26 ChIP-Seq data (GSM2026873) were obtained from the Gene Expression Omnibus (GEO) database. mRNA sequencing data of 530 ccRCC tissues and 72 benign renal tissues, including gene expression data and clinical information, were sourced from the TCGA database. CheckMate-025 cohorts of advanced ccRCC patients treated with Nivolumab (anti-PD-1) and everolimus (mTOR inhibitor) therapy were obtained from the published article.[14] The ccA and ccB molecular subtypes of ccRCC were defined as previously reported.[15]

Patients and Tissue Samples

An ccRCC tissue microarray for evaluating ACE expression was purchased from Shanghai Outdo Biological Technology (Shanghai, China). Clinicopathologic information was documented for all cases. Additionally, 25 pairs of fresh ccRCC cancer tissues and adjacent normal tissues were used for qPCR and Western blot analysis. All samples were accessed with informed consent from patients.

The study was conducted in accordance with the principles of the Declaration of Helsinki and was approved by the Changzhou Second People's Hospital and the Nanjing Medical University Ethics Committee.

Gene Co-Expression Profiling and GSEA

Co-expressed genes with ACE in the TCGA-ccRCC dataset were identified using Pearson's correlation analysis. The results were displayed in volcano plots and heat maps. The LinkInterpreter module was used to perform Gene Ontology Biological Process (GO_BP) and Kyoto Encyclopedia of Genes and Genomes (KEGG) pathway analyses. Gene Set Enrichment Analysis (GSEA) was conducted using the curated gene sets from the MSigDB, derived from KEGG and Hallmark collections. GSEA was run in pre-ranked mode using classic metrics and 1000 permutations.

Cell Culture, Transfection, and Lentiviral Infection

The ccRCC cell lines (OS-RC-2 (RRID:CVCL_1626) and A498 (RRID:CVCL_1056)) and HEK293T (RRID:CVCL_0063) cells were obtained from the Cell Bank of the Chinese Academy of Sciences (Shanghai, China). All cells were grown in DMEM supplemented with 10% FBS (Gibco, USA). Plasmid constructs or siRNAs were transfected using Lipofectamine 3000 (Invitrogen, USA) according to the manufacturer's protocol. Lentiviruses expressing shRNAs targeting ACE (sh#ACE) and negative control shRNA (LV-NC) were constructed using the pLKO.1 lentiviral vector. Overexpression lentiviruses expressing ACE were constructed using the PWPI lentiviral vector. All lentiviruses were provided by GENECHEM (Shanghai, China). Detailed target sequences are listed in Supplementary Table 1.

RNA Isolation and Real-Time PCR

Total RNA was extracted using the RNA-Quick Purification Kit (ES Science, China), and cDNA was synthesized using the HiScript II Q-RT SuperMix kit (Vazyme, China). qPCR was performed using SYBR Green PCR master mix (Vazyme, China). Each sample was tested in triplicate. Data were quantified using the $2^{-\Delta\Delta Ct}$ method. Primers are described in Supplementary Table 2.

Western Blotting

For Western blot analysis, cells were lysed in RIPA buffer supplemented with a protease inhibitor cocktail (Beyotime Biotechnology, China). Proteins from each sample were loaded, separated, and transferred to PVDF membranes. Immunoreactive bands were visualized using the ECL Western blot kit (ES Science, China). Antibodies used are listed in Supplementary Table 3.

Cell Proliferation Assay

Cell proliferation levels were determined using the CCK-8 kit (Dojindo, Japan) according to the instruction manual. Optical density was measured at 450 nm using a multifunctional microplate reader (Biotek, USA).

Cell Migration and Invasion Assays

Migration assays were conducted using the Transwell system (Corning, USA) according to the manufacturer's instructions. For invasion assays, the upper chamber was coated with Matrigel (Corning, USA). After 24 hours, cells were fixed, stained with 0.1% crystal violet, and counted under a microscope. Data were collected from at least three independent experiments.

Immunohistochemistry (IHC) and Immunofluorescence (IF) Staining

IHC experiments were conducted following established protocols.[16] Tissue sections were incubated with primary antibodies overnight at 4°C, followed by secondary antibodies at room temperature. IHC staining was independently assessed by three experienced pathologists. A semiquantitative scoring system was employed, calculating the staining index (0–12) by multiplying the staining intensity by the proportion of positive cells.

Immunofluorescence (IF) Staining

IF staining was performed by fixing slides with 4% paraformaldehyde and permeabilizing with 0.1% Triton X-100. Slides were blocked with 10% goat serum and incubated overnight at 4°C with the primary antibody. After washing in PBS, slides were stained with fluorophore-coupled secondary antibodies for 1 hour at room temperature, followed by DAPI staining. Slides were observed under fluorescence microscopy.

ACE Activity Assay

ACE activity in adjacent normal tissues and cccRCC tumor samples was measured using the ACE Activity Assay Kit (CS0002, Sigma-Aldrich, USA), following the manufacturer's protocol. Briefly, 20 μg of tissue was homogenized by grinding in liquid nitrogen and then diluted in 40 μL of assay buffer. The homogenate was centrifuged to remove cell debris, and 50 μL of substrate was added. Fluorescence was measured with excitation at 320 nm and emission recorded at 420 nm.

Chromatin Immunoprecipitation (ChIP) Assay

The ChIP assay was conducted following the Cold Spring Harbor protocol.[17] Briefly, cells were treated with 1% formaldehyde at room temperature for 10 minutes to cross-link DNA. After sonication, the cross-linked chromatin was precleared with A/G-agarose beads and immunoprecipitated with an anti-FOXO1 antibody overnight at 4°C. IgG was used as the negative control. Specific primers for amplifying the target sequence of the human ACE promoter are provided in Supplementary Table 4.

Cignal Finder Reporter Array

To investigate the pathways regulated by ACE, the Cignal Finder Pathway Reporter Array (Qiagen, Germany) was used following the manufacturer's instructions. Briefly, 50 μL of cell suspension (5×10^4 cells) was seeded into each well after the preparation of complex formation and incubated for 12 hours. After incubation, the medium was replaced with complete growth medium. A dual luciferase assay was performed using the Dual-Glo® Luciferase Assay System (Promega, USA), and the results were analyzed with a Glomax-multi Luminometer (Promega, USA).

Luciferase Reporter Assay

The human ACE promoter was cloned into the pGL3-basic vector (Promega, USA). Cells were seeded in 24-well plates and transfected using Lipofectamine 3000 (Invitrogen, USA) following the manufacturer's protocol. The pRL-TK plasmid expressing Renilla luciferase served as a control. After incubation, luciferase activity was measured and analyzed.

Seahorse Assay

Extracellular acidification rate (ECAR) and oxygen consumption rate (OCR) were determined with a Seahorse XF96 Analyzer (Agilent Technologies, USA) following protocols recommended by the manufacturer. Briefly, individual groups of cells (1×104 cells/well) were seeded in triplicate in an XF 96-well microplate and used to measure ECAR and OCR at different time points by adding indicated reagents. The data were recorded automatically.

Animal Experiments

All animals were housed in pathogen-free facilities. The animal experimental procedures were performed in accordance with the Guide for the Care and Use of Laboratory Animals published by the National Institutes of Health (NIH Publication, 8th edition, 2011) and approved by the Nanjing Medical University Animal Care and Use Committee. To establish a subcutaneous xenograft model, ccRCC cells (1×10^6) were suspended in 100 μL PBS and injected subcutaneously into both flanks of 5-6-week-old male athymic nude mice (BALB/c) (n=4 mice/group). Tumor growth was measured using an electronic caliper, and tumor volume (V) was calculated using the formula: V = 0.5 × length × width^2. At the end of the experiments, all tumors were excised, weighed, and stored for subsequent histological and biochemical analyses.

For the renal orthotopic tumor model, BALB/c male nude mice (5–6 weeks old) were anesthetized with isoflurane (2.0–3.0%) mixed with air. A total of 1×10^6 ccRCC cells in 10 μL PBS were injected into the subcapsular space of the right kidney. Mice were monitored until one group reached total mortality or until 7 weeks after tumor cell injection. All mice were then sacrificed, and the orthotopic xenograft tumors were extracted and weighed.

Statistical Analysis

All data shown in graphs are expressed as means ± standard deviation (SD). Calculations were performed using SPSS (Version 20.0, IBM, USA) and GraphPad Prism 8 (GraphPad, USA). Differences between two groups were assessed using a two-tailed unpaired Student's *t*-test. One-way ANOVA was used for comparisons among multiple groups. Survival probability was calculated using the Kaplan-Meier method. Statistical significance was denoted as follows: *P < 0.05, **P < 0.01, ***P < 0.001, and ****P < 0.0001. n.s., not significant.

Results

Decreased ACE Expression Linked to Malignant Clinical-Pathological Characteristics in ccRCC

To begin understanding the role of RAAS (ACE, AGTR1, AGTR2, REN, AGT and ACE2) in ccRCC, we first assessed their levels in the CPTAC samples (Mass spectrometry based proteomic profiling of 110 ccRCC cases including 84 paired normal cases). Among the six candidates, ACE was selected for further study due to its most differential expression between tumor and adjacent normal tissues (Figure 1A). Moreover, protein-protein interaction (PPI) network analysis identified ACE as a hub gene in the RAAS components (Figure S1A). Additional analysis of the Pan-CPTAC datasets revealed that ACE was down-regulated in most malignant tumors, particularly in ccRCC, which showing significant changes in protein expression (more than a 20-fold decrease relative to normal tissue), indicating ACE may play a direct role in cancer progression (Figure S1B). This was further confirmed by comparing paired tumor and adjacent normal samples from three independent cohorts (Figure 1B-D). To assess the clinical significance of ACE in ccRCC, the TCGA dataset was analyzed. Interestingly, ACE down-regulation increased with higher histological grade, clinical stage, pathological grade, and distant metastasis (Figure 1E-H). It was also showed ACE expression enriched in the ClearCode34 molecular subtype A (ccA), indicating a better prognosis (Figure S1C). Indeed, Kaplan–Meier analysis showed that high ACE expression was significantly associated with better overall survival, disease-specific survival, and progression-free interval (Figure 1I-K). Moreover, patients in advanced stages or grades with low ACE expression had significantly poorer overall survival compared to those with high ACE expression (Figure S2). Collectively, ACE is downregulated in ccRCC tissues and is closely related to clinical prognosis.

To validate the results from the database, we first examined the mRNA levels of ACE in 25 paired fresh tissues from our clinical facility, and found that 64% of the adjacent normal tissues showed high ACE expression, while only 12% of the ccRCC tissues did, with the difference being statistically significant (Figure 1L). Moreover, down expression of ACE protein expression was detected in ccRCC tissues of six representative patients (Figure 1M). Consistently, enzymatic activity of ACE was also reduced in tumor samples (Figure 1N). Besides, we measured ACE protein expression by immunohistochemistry (IHC) staining in a tissue microarray (TMA) containing 71 ccRCC cases and 17 adjacent normal tissues. IHC data showed that ACE expression levels were downregulated in tumor tissues compared to normal tissues

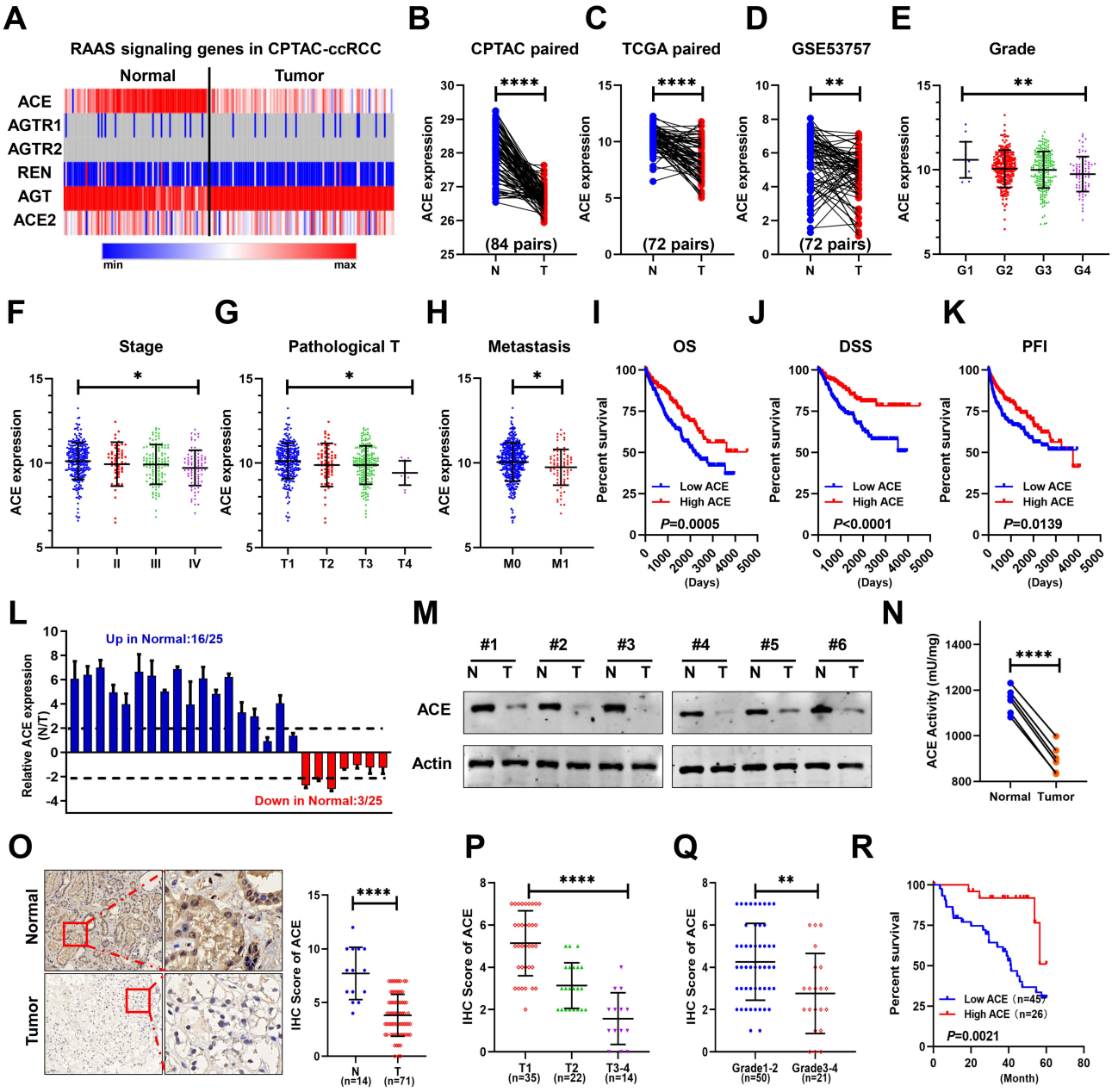

Figure 1 Low expression of ACE was associated with poor prognosis in ccRCC patients. (**A**) The protein expression of RAAS signaling genes in CPTAC-ccRCC dataset. (**B-D**) ACE protein or mRNA of levels were compared between ccRCC tumors and paired normal tissues from the CPTAC (**B**), TCGA (**C**) and GEO (**D**) database. (**E-H**) ACE mRNA levels were assessed in patients with ccRCC grades (**E**), stages (**F**) and Pathological T stage (**G**) using TCGA database data. (**H**) Analysis of ACE expression in metastatic data. (**I-K**) Kaplan-Meier curve showing Overall survival (**I**), Disease specific survival (**J**) and Progression free interval (**K**) in high- and low-ACE in ccRCC. (**L**) The mRNA levels of ACE in 25 ccRCC tissues and adjacent normal tissues. (**M**) ACE protein levels were assessed in 6 ccRCC tumor and para cancerous tissue samples. (**N**) ACE activity assay was detected in above samples. (**O**) Representative IHC staining (left) and H-score (right) for ACE in ccRCC tissues and matched para-tumor tissues. (**P**) IHC score between patients with different T stage. (**Q**) IHC score between patients with different Fuhrman grade. (**R**) Kaplan–Meier survival curve analysis the expression level of ACE and the prognosis of ccRCC patients. n.s., not significant; *P < 0.05; **P < 0.01 and ****P < 0.0001.

(Figure 1O). Furthermore, ACE downregulation was significantly associated with pathological tumor stage and Fuhrman grade (Figure 1P and Q). We also analyzed the overall survival of ccRCC patients from TMA by Kaplan–Meier analysis. The results indicated that patients with high ACE expression had longer survival times than those with low ACE expression (Figure 1R). Then, we further examined whether ACE is an independent prognostic factor based on univariate and multivariate Cox analysis. We found that the following factors were significantly related to OS: tumor stage and ACE

expression level (Supplementary Table 5 and 6). Therefore, low ACE expression could serve as an independent poor prognostic marker for ccRCC patients.

ACE Inhibits Malignant Biological Functions of ccRCC in vitro and in vivo

To elucidate ACE's role in ccRCC progression, we constructed ACE overexpression and knockdown cells (OS-RC-2 and A498) and validated them via Western blot (Figure 2A and B). ACE overexpression hindered proliferative activity in both cell lines compared to controls, while ACE knockdown increased cell proliferation (Figure 2C and D). Moreover, ACE overexpression disrupted migratory and invasive activities in Transwell assays, contrasting with ACE loss (Figure 2E and F). We also determined whether altered ACE levels influence glycolytic metabolism in ccRCC cells by measuring both the oxygen consumption rate (OCR) and extracellular acidification (ECAR). Indeed, ECAR, which indirectly reflects glycolytic capacity and glycolysis, was decreased when ACE was overexpressed or increased after ACE was knocked down (Figure 2G-J). In contrast, ACE overexpression increased OCR, whereas cells with ACE inhibition reduced OCR, indicating that reconstitution of ACE in ccRCC cells restores mitochondrial respiration at least partially (Figure 2K-N).

To evaluate the role of ACE in ccRCC tumorigenesis, a xenograft tumor model was established through the subcutaneous implantation of nude mice with ccRCC cells (Figure 2O). The results showed that ACE overexpression significantly inhibited tumor growth and tumor weight (Figure 2P and Q), which were in line with the results in vitro. To further demonstrate the active role of ACE in ccRCC in vivo, we employed an orthotopic xenograft model generated by injecting OS-RC-2 cells into the renal capsules of nude mice (Figure 2R). The tumor weight of the ACE overexpression group was evidently lower compared to the control group (Figure 2S). In addition, mice in the control group had significantly worse prognosis than those administered with ACE (Figure 2T). These findings reinforce the notion that ACE correlates with a favorable prognosis in ccRCC patients.

ACE Co-Expressed Genes are Regulated in Cancer-Related Cascades

To explore the potential downstream target genes of ACE, we then used the function module to explore the co-expressed genes related to ACE from ccRCC samples in TCGA. The volcano plot showed that 5392genes (red dots) were significantly positively correlated with ACE expression, while 3755 genes (green dots) were significantly negatively related (FDR<0:01, Figure 3A). Heat maps displayed the top 50 positively and negatively associated genes with ACE (FigureS3A and S3B), and correlation coefficients and P values were detailed in Supplementary Table 7. To confirm this differential expression and assess ACE's clinical significance, the top 1000 genes related to ACE plus and minus were performed Gene Ontology (GO) and KEGG pathway analyses. The results indicated that ACE co-expressed genes were mainly associated with epithelial-mesenchymal transition (EMT) and multiple cancer related signaling pathway (Figure S3C and S3D).

To narrow down detailed signaling pathways affected by ACE in ccRCC, Cignal Finder RTK signaling 10-Pathway Reporter Array was performed. Using a more stringent criteria (P<0.01) for both ACE overexpression and down-regulation groups, PI3K-AKT signaling emerged as the most heavily affected pathway, which was consistent with KEGG analyses (Figure 3B, C and S3D). Similarly, Gene set enrichment analysis (GSEA) revealed that the gene sets related to ccRCC or AKT signaling negatively correlated with ACE expression (Figure 3D). Further immunoblotting analysis demonstrated that ACE overexpression inhibited the phosphorylation of AKT and GSK-3β (a direct substrate of pAKT), while the opposite results were observed in knockdown of ACE (Figure 3E). What's more, FOXO1, a major substrate of AKT, was closely and positively correlated with the expression of ACE (Figure 3E). Given that AKT phosphorylation induces localization of FOXO proteins, we next examined the impact of FOXO1 cellular localization with or without ACE expression. As expected, immunofluorescence showed that FOXO1 protein level was simultaneously upregulated in ectopic overexpression of ACE, while inducing its nuclear expression (Figure 3F). To validate these results, luciferase reporter assay was performed to determine whether ACE alteration could influence the transcriptional activity of FOXO1. Consistently, ACE overexpression resulted in promotion of FOXO1 response element activity in a dosage-dependent manner (Figure 3G).

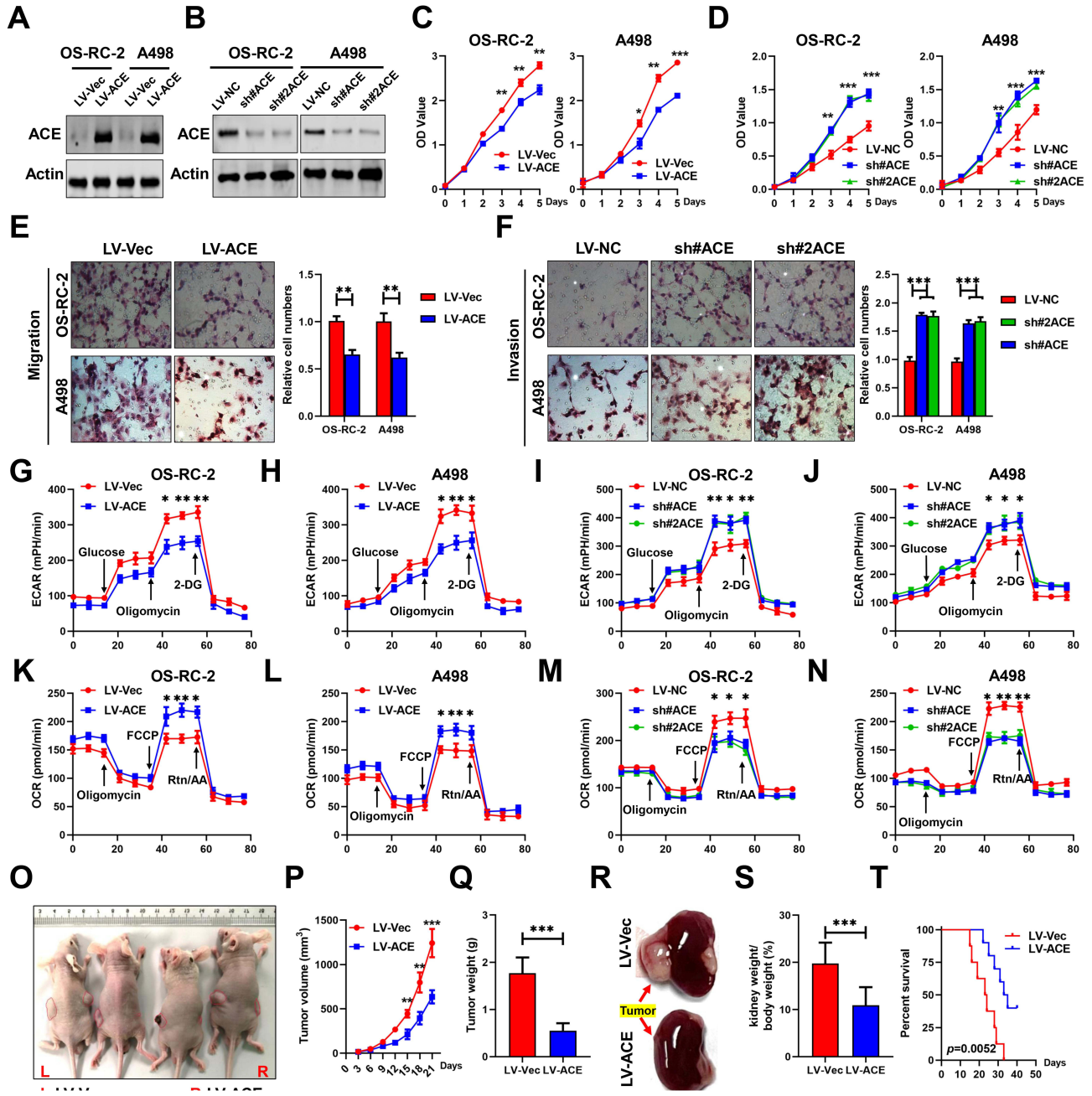

Figure 2 ACE is a tumor suppressor gene with prognostic value. (**A-B**) Reintroducing ACE (**A**) or knockdown of ACE (**B**) efficiency in ccRCC cells was confirmed via Western immunoblotting. (**C**) CCK-8 assays were used to assess ccRCC cell growth with or without exogenous ACE. (**D**) CCK-8 assays were used to assess ccRCC cell growth in the presence or knockdown of ACE. (**E**) Migration assay detected with or without exogenous ACE. (**F**) Invasion assay detected with presence or knockdown of ACE. (**G-J**) The ECAR of indicated cells was measured with the XF24 Seahorse Analyzer. (**K-N**) The OCR of indicated cells was measured with the XF24 Seahorse Analyzer. (**O**) Representative images of the subcutaneous tumors in the bilateral flanks of nude mice (left flank, control OS-RC-2 cells; right flank, OS-RC-2 with exogenous ACE). (**P-Q**) Tumor volumes (p) and tumor weights (q) of the two groups were shown. (**R**) Representative images of renal orthotopic tumors as indicated groups. (**S**) Kidney weight/body weight expressed as a percentage rate. (**T**) Comparisons of the OS curves of mice between indicated groups. *P < 0.05; **P < 0.01 and ***P < 0.001.

ACE Inhibition of ccRCC Progression by Disrupting the AKT-FOXO1 Signaling Pathway

Given the vital role of the AKT-FOXO1 axis in tumor metastasis, we investigated whether ACE is closely involved. GSEA analysis of TCGA data revealed that ACE expression is enhanced in adherent junctions and focal adhesion (Figure 3H and S3C). We next detected the expression of EMT markers (E-cadherin and N-cadherin) via immunofluorescent staining of xenograft tumor samples, which showed increased E-cadherin and decreased N-cadherin expression in

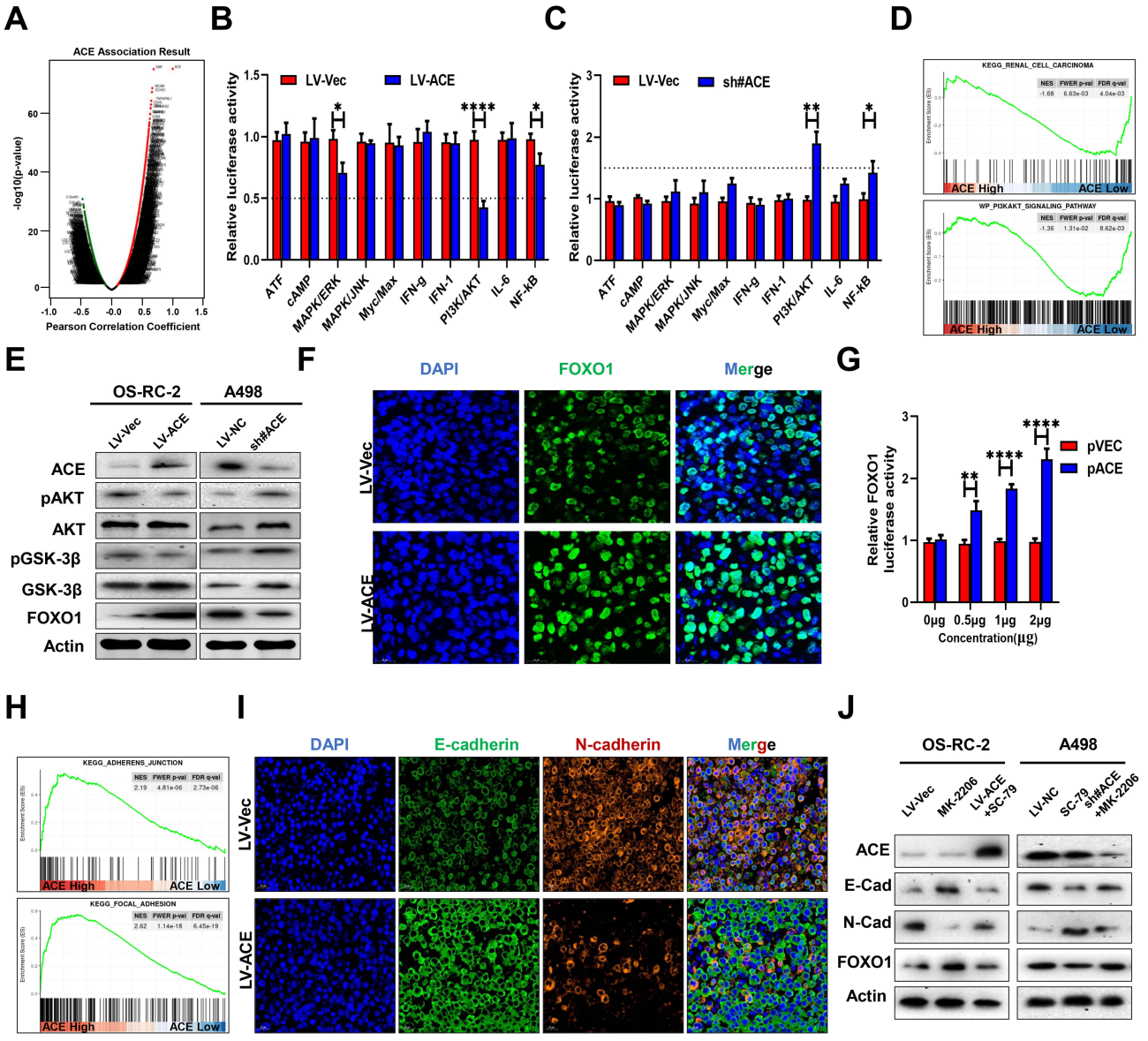

Figure 3 Co-expressed genes regulated with ACE and accompanied by EMT. (**A**) The correlation between ACE and genes differentially expressed in ccRCC was evaluated by a Pearson test. (**B-C**) Cignal Finder Reporter Array was conducted in A498 cells transfected with ACE (**B**) or knockdown of ACE (**C**). (**D**) GSEA for gene signatures of ccRCC (upper panel) and AKT (down panel) signaling. (**E**) Western blots were performed to verify the effects of altered ACE expression on the expression of specific proteins related with AKT-FOXO1signaling. (**F**) Immunofluorescence analysis of FOXO1 level in A498 cells with or without exogenous ACE. (**G**) Dual Luciferase reporter assays were performed to determine whether ACE could affect the FOXO1 activity. (**H**) The GSEA plot shows enrichment of EMT-related pathways. (**I**) Immunofluorescence was used to detect the protein levels of EMT-related factors. (**J**) Expressions of EMT-related markers and FOXO1 in the indicated ccRCC cells were detected by Western blot assay. *P < 0.05; **P < 0.01 and ****P < 0.0001.

the ACE overexpression group (Figure 3I). These findings support ACE as a potential target for cancer metastasis therapy. What's more, treatment with MK-2206, an AKT inhibitor, induced an epithelial-like molecular phenotype and increased FOXO1 expression in OS-RC-2 cells. Conversely, ACE downregulation of mesenchymal-like markers was restored by adding SC-79, an AKT activator (Figure 3J left). In A498 cells, treatment with SC-79 induced E-cadherin, FOXO1 decreasing and N-cadherin increasing. Alternatively, adding MK-2206 led to in turn results in dismissal of shACE-mediated E-cadherin, FOXO1 and N-cadherin change (Figure 3J right). Additionally, biological experiments showed that AKT inhibitor hindered proliferation, migration, invasion and aerobic oxidation capacities similar to ectopic ACE expression, while AKT activator reversed the inhibitory effects of ACE on ccRCC cell phenotype (Figure 4A-P). These results suggest that ACE acts as a tumor suppressor gene dependent on inhibiting AKT-FOXO1 signaling.

https://doi.org/10.2147/BTT.S485178 DovePress

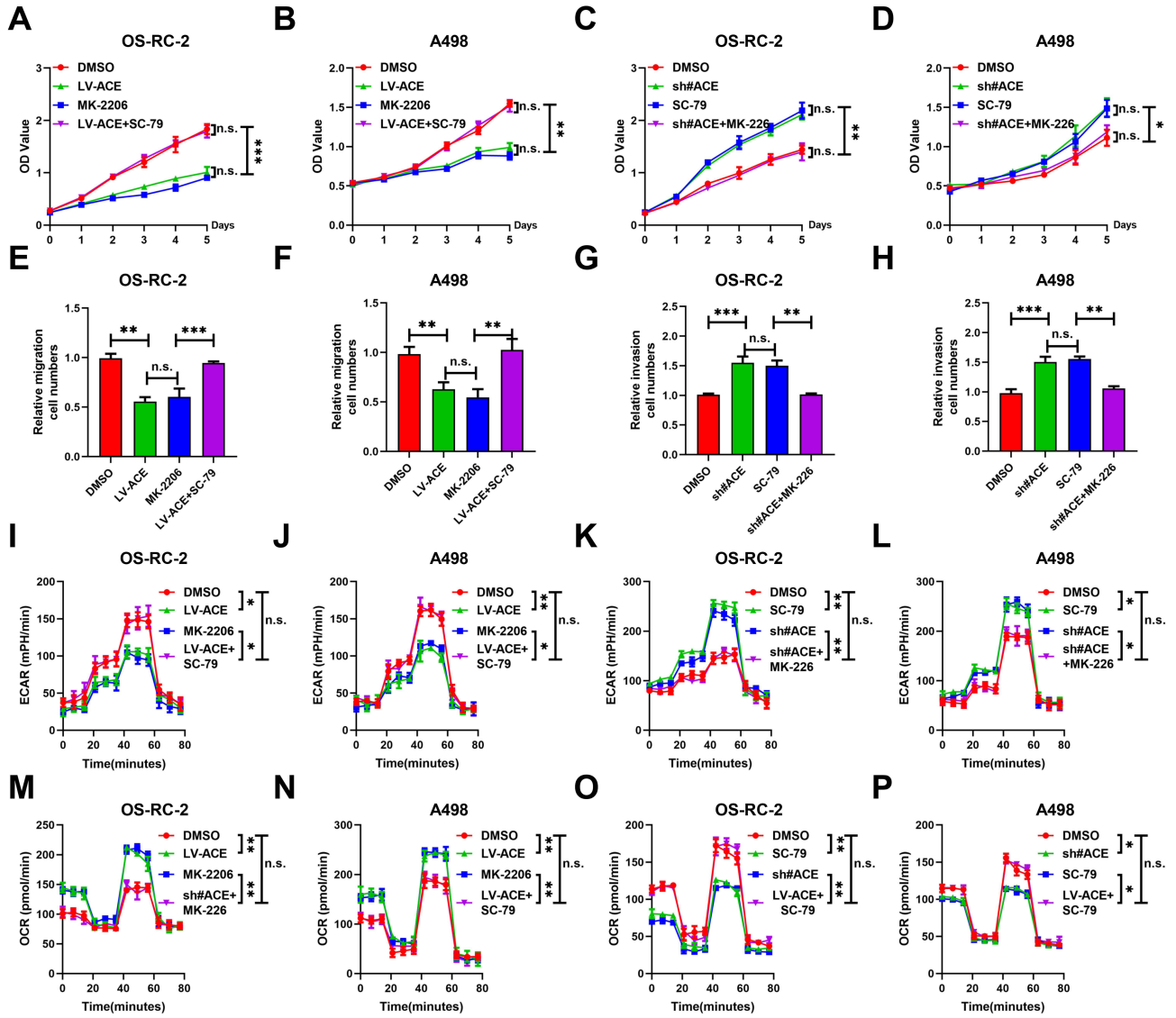

Figure 4 ACE is important for AKT-FOXO1 signaling in ccRCC cells. (**A-D**) Proliferation in the indicated cell groups was evaluated by CCK-8 assay. (**E-H**) Migration (**E** and **F**) and invasion (**G** and **H**) abilities in the indicated cell groups were evaluated by Transwell assay. (**I-L**) The ECAR of indicated cells was measured with the XF24 Seahorse Analyzer. (**M-P**) The OCR of indicated cells was measured with the XF24 Seahorse Analyzer. n.s., not significant; *P < 0.05; **P < 0.01 and ***P < 0.001.

ACE Enhanced the Anticancer Effects of Everolimus

Recent reports indicate that RAAS may participate in tumor chemotherapy and immunotherapy.[18] Therefore, we analyzed the correlation between ACE expression and clinical outcomes in the Phase 3 CheckMate-025 study (involving nivolumab or everolimus treatment in advanced ccRCC). The Kaplan–Meier analyses showed that ACE expression has predictive value for clinical outcomes in ccRCC patients treated with everolimus, but not in the nivolumab treatment group (Figure 5A and Figure S4A-C). Furthermore, subgroup analysis found that the high ACE expression group had better IMDC or MSKCC prognostic scores (Figure 5B and C). Further enrichment plots from GSEA showed that mTOR pathway gene signatures were suppressed in patients with high ACE expression (Figure 5D). These results led us to speculate that ACE might synergize with everolimus. To test this possibility, we examined the effect of ACE and everolimus on the biological function of ccRCC cells. The combination of ACE and everolimus significantly suppressed cell viability compared to each treatment alone (Figure 5E and F). Similarly, combined therapy significantly suppressed the migratory and invasive capacities of ccRCC cells compared to monotherapy (Figure 5G-J). Moreover, ECAR was dramatically reduced and OCR was significantly enhanced in cells treated with both ACE and everolimus, indicating

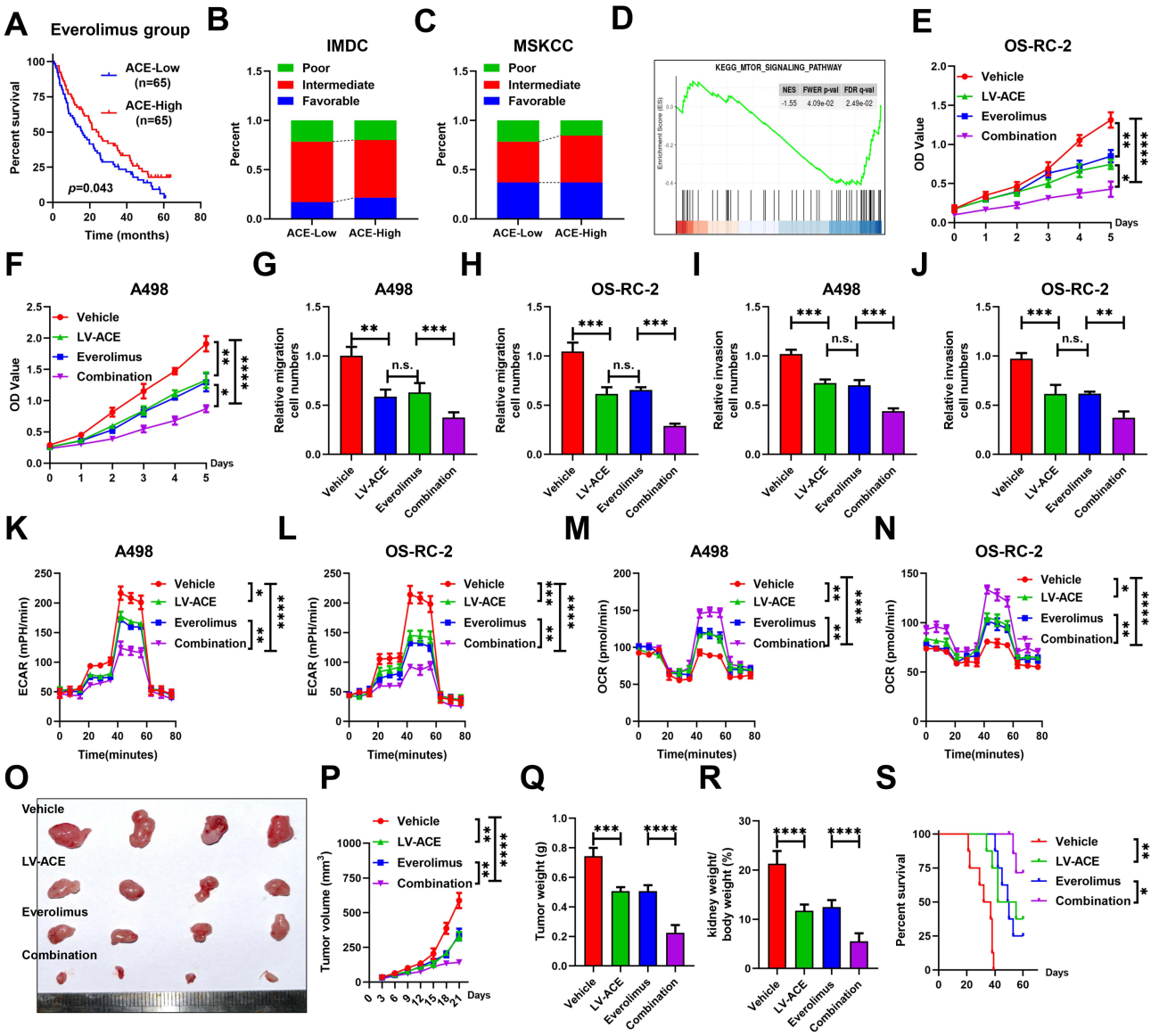

Figure 5 ACE enhances the anti-cancer effects of everolimus. (**A**) Kaplan–Meier survival curve analysis the expression level of ACE and the prognosis in checkmate 025 everolimus treatment group. (**B-C**) The distribution of ACE expression as IMDC (**B**) and MSKCC (**C**) risk score. (**D**) GSEA for gene signatures of mTOR signaling. (**E-F**) Proliferation in the indicated cell groups was evaluated by CCK-8 assay. (**G-J**) Migration (**G** and **H**) and invasion (**I** and **J**) abilities in the indicated cell groups were evaluated by Transwell assay. (**K-L**) The ECAR of indicated cells was measured with the XF24 Seahorse Analyzer. (**M-N**) The OCR of indicated cells was measured with the XF24 Seahorse Analyzer. (**O**) Representative images of the subcutaneous tumors treated with indicated regimens. (**P-Q**) Tumor volumes (**P**) and tumor weights (**Q**) of the indicated groups were shown. (**R**) Kidney weight/body weight expressed as a percentage rate. (**S**) Comparisons of the OS curves of mice between indicated groups. n.s., not significant; *P < 0.05; **P < 0.01; ***P < 0.001 and ****P < 0.0001.

a strong synergistic effect (Figure 5K-N). Next, we tested these effects in vivo. As shown in Figure 5O, tumors in mice bearing OS-RC-2 cells responded effectively to everolimus administration. Likewise, combined treatment with exogenous ACE expression and everolimus showed the strongest tumor growth suppression in mice (Figure 5P and Q). Additionally, an orthotopic xenograft model demonstrated that combined therapy significantly reduced tumor weight and prolonged survival time compared to monotherapy (Figure 5R and S). In conclusion, these results demonstrate that ACE combined with everolimus has a synergistic anti-tumor effect on ccRCC.

ZBTB26 Transcriptional Regulation of ACE in ccRCC

The importance of ACE in ccRCC prompted us to identify the regulatory mechanism responsible for its decreased expression. Through in silico analyses of ChIP-seq dataset Cistrome, a list of highly correlated target genes (Score ≥ 0.6) was found (Figure 6A and Supplementary Table 8). Among them, ZBTB26 was the most highly correlated potential regulator which not

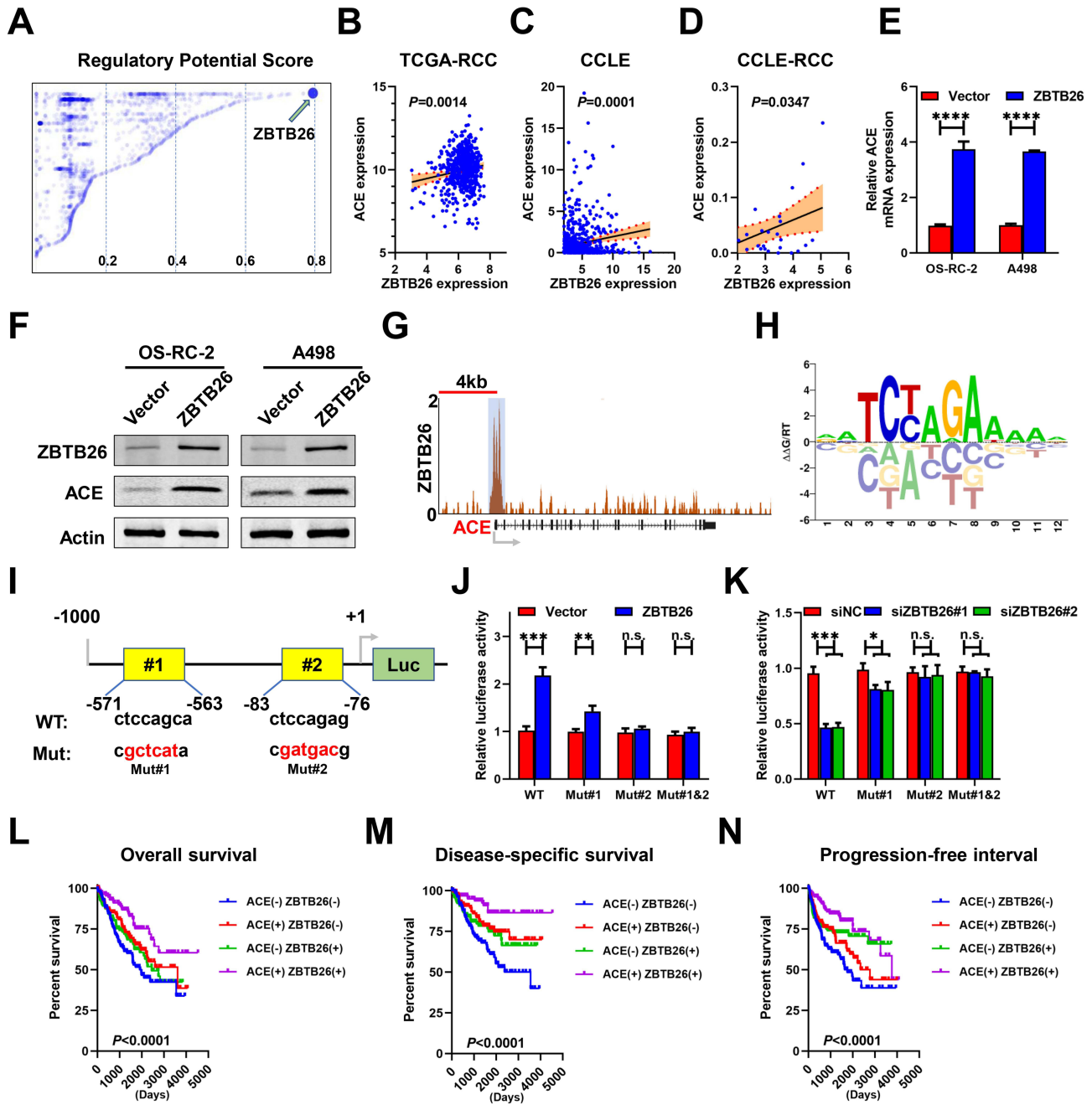

Figure 6 ACE is a direct target of ZBTB26 in ccRCC. (**A**) Predicted potential transcription factors that could bind promoter of ACE. (**B-D**) Correlation of ZBTB26 and ACE mRNA in TCGA (**B**), CCLE (**C**) and only CCLE-ccRCC (**D**) data were analyzed. (**E**) Relative mRNA levels of ACE in control cells and in transfected with ZBTB26 cells. (**F**) The protein level of ACE was assessed in control cells and in transfected with ZBTB26 cells. (**G**) ChIP-seq assays showing the ZBTB26 enrichment peak at the ACE promoter region. (**H**) Multiple sequence alignment of predicted ZBTB26 binding sites. (**I**) Schematic diagram of wide type and site-directed mutant plasmids. (**J-K**) ChIP-PCR were performed to detect the enrichment of ZBTB26 on the ACE promoter in indicated HKE293T cells. (**L-N**) Kaplan–Meier analysis of prognostic value that combining ZBTB26 and ACE levels in TCGA-ccRCC samples. n.s., not significant; *P < 0.05; **P < 0.01; ***P < 0.001 and ****P < 0.0001.

previously validated in kidney cancer. Therefore, we determined whether the expression of ACE is regulated by ZBTB26. Indeed, the significantly positive correlation was obtained in TCGA-ccRCC, Cancer Cell Line Encyclopedia (CCLE) pan-cell, and ccRCC cell line data respectively (Figure 6B-D). Similar results were also observed that overexpression of ZBTB26 was accompanied a marked increase in both ACE mRNA and protein levels (Figure 6E and F). Moreover, the potential binding of ZBTB26 were identified on the core promoter region (−1000bp~100bp) of ACE in the published ChIP-Seq data (Figure 6G). Combining the ZBTB26 binding sites sequence, we constructed two mutant plasmids to explore which site mediated the

transcriptional effect of ZBTB26 on ACE (Figure 6H and I). Further luciferase assay indicated that Mut2 totally lost reporter activity, whereas Mut1 retained large percent of activity, suggesting that the ZBTB26-binding element proximal to the transcription starting site is the major binding site for the ACE promoter (Figure 6J and K). More importantly, Kaplan–Meier survival analysis revealed that ACE-high/ZBTB26-high subgroup had the best overall survival, disease-specific survival, and progression-free interval rate, while the ACE-low/ZBTB26-low subgroup had the worst outcome (Figure 6L-N). Together, our results demonstrated ZBTB26 transcriptionally regulates the expression of ACE and played a critical role in disease progression in renal cell carcinoma.

Discussion

The urgency to develop novel diagnoses and therapies for ccRCC is evident due to the limited treatment options and poor clinical outcomes. Our previous study highlighted the pivotal role of aberrant regulation of key enzymes or regulatory factors in ccRCC progression [19,20]. While the renin-angiotensin-aldosterone system (RAAS) is crucial for various physiological processes, its involvement in cancer, particularly ccRCC, remains poorly understood. In this study, we focused on one core of the RAAS component—ACE, has detected enrichment in normal kidney tissues compared to in ccRCC samples. Additionally, clinical data aligns with these observations, confirming that lower ACE expressions are closely correlated with higher grades and stages of ccRCC, as well as worse patient survival outcomes. Therefore, investigating ACE may offer a breakthrough in tumor therapy.

Progression of ccRCC is usually associated with tumor growth and metastasis.[21] The in-vitro experiments we performed confirmed that ACE inhibited ccRCC cell growth. Besides, ACE also hindered the metastatic ability of ccRCC by inhabiting cells to migrate and invade, which further validated in animal models. Our findings were consistent with previous studies that ACE reduce tumor growth in melanoma and lung cancer [22,23]. EMT is a classical and acknowledged driver of metastasis, which is regulated by different activators at different levels.[24] Our systematic transcriptome analysis performed in TCGA-ccRCC dataset showed that ACE expression strongly correlates with motility pathways, such as Adherents junction and Focal adhesion. Further investigation showed ACE stimulated the process by increasing the expression of the epithelial marker E-cadherin and decreasing the level of the mesenchymal markers N-cadherin. This is consistent with the finding in other types of malignancies [25,26].

Aerobic glycolysis, also known as the Warburg effect, is a hallmark metabolic feature of ccRCC.[27] This process fulfills the energetic and biosynthetic demands required for the sustained growth and metastasis of cancer cells, while also modulating the tumor microenvironment by promoting angiogenesis and, in some cases, facilitating tumor thrombus formation [28,29]. In this study, we demonstrate that ACE increases the oxygen consumption rate, suggesting that the reconstitution of ACE in ccRCC cells restores mitochondrial respiration. Additionally, our renal orthotopic tumor model suggests that ACE may reduce tumor thrombus formation (data not shown). Given that approximately 15% of RCC patients present with venous tumor thrombus in the renal vein or inferior vena cava,[30] further investigation into ACE's role in this process could provide valuable biological and clinical insights for the treatment of RCC.

Abnormal AKT activation is a hallmark of tumor progression in various cancers, including ccRCC.[31] GSK3β is a substrate of AKT. AKT can phosphorylate GSK3β, inhibiting its activity. GSK3β phosphorylates various substrates and mediates multiple biological.[32] FOXO1, a well-established tumor suppressor, is an essential catalytic substrate of AKT.[33] Here, our results of Cignal Finder Reporter Arrays and Western blots also demonstrated that both pGSK3β and pAKT levels were decreased when ACE overexpression. More importantly, FOXO1, was also greatly increased and translocation into nucleus due to ACE overexpression.

In recent years, mTOR, a key downstream protein kinase of the PI3K/AKT signaling pathway, has been recognized as "master switch" protein in cancer cells to modulate metabolism, cell cycle, and metastasis [34,35]. However, clinical trials on ccRCC patients largely failed when mTOR inhibitors, everolimus, was used as a single agent [36,37]. In view of this obstacle, exploring treatment strategies to improve targeted therapy response and survival is urgent. For the first time, we report that exogenous expression of ACE combined with everolimus has synergistic inhibit tumor development and provide a novel strategy for ccRCC treatment. Nonetheless, multiple mechanisms are likely involved in the combined ACE and everolimus treatment, warranting further investigation.

The reason behind the decrease in ACE expression in ccRCC remains elusive. Our correlative analysis and ChIP-seq profiles indicated that ACE may as a direct target of ZBTB26. Recently, increasing attention has been paid to ZBTB proteins, which are the family proteins of nuclear transcription factors.[38] These genes could participate in the regulation of multiple gene transcription via binding to corresponding cis-regulatory elements. Notably, many members of them have been reported to play important roles in the development of multiple cancers, such as ZBTB9, ZBTB27 and ZBTB7A [39–41]. In the present study, we found high ACE level is tightly correlated with ZBTB26 expression both in mRNA and protein levels. Mechanistically, ChIP assay and luciferase assay uncovered that ZBTB26 directly binds to the promoter of ACE and leading to its transactivation.

In summary, our findings investigated the roles and mechanisms of ACE in ccRCC (Figure S5). ACE inhibits the growth and metastasis of ccRCC cells in vitro and in vivo by promoting FOXO1 expression, which is the downstream target of PI3K-AKT pathway. Thus, this research suggest that ACE may be a promising target for new therapeutic strategy in ccRCC.

Abbreviation

RAAS, renin-angiotensin-aldosterone system; ccRCC, Clear-cell renal cell carcinoma; ACE, angiotensin-Converting Enzyme; EMT, epithelial-mesenchymal transition; CPTAC, clinical proteomic tumor analysis consortium; GEO, gene expression omnibus; ChIP, chromatin immunoprecipitation; TMA, tissue microarray; OCR, oxygen consumption rate; ECAR, extracellular acidification rate.

Data Sharing Statement

All datasets generated for this study are included in the manuscript.

Acknowledgments

We thank TCGA, CPTAC, GEO databases, and UCSC Genome Browser for free use.

Author Contributions

All authors made a significant contribution to the work reported, whether that is in the conception, study design, execution, acquisition of data, analysis and interpretation, or in all these areas; took part in drafting, revising or critically reviewing the article; gave final approval of the version to be published; have agreed on the journal to which the article has been submitted; and agree to be accountable for all aspects of the work.

Funding

This work was supported by the National Natural Science Foundation of China (Grant No. 82203698), the Sailing Program of Shanghai Science and Technology Commission (Grant No. 22YF1425000) and Project of Changzhou Second People's Hospital affiliated to Nanjing Medical University (Grant No. 2021K007).

Disclosure

The authors declare no conflict of interest.

References

1. Jonasch E, Walker CL, Rathmell WK. Clear cell renal cell carcinoma ontogeny and mechanisms of lethality. *Nat Rev Nephrol*. 2021;17:245–261. doi:10.1038/s41581-020-00359-2
2. McKay RR, Bosse D, Choueiri TK. Evolving systemic treatment landscape for patients with advanced renal cell carcinoma. *J Clin Oncol*. 2018;36 (36):3615–3623. doi:10.1200/JCO.2018.79.0253
3. Longo R, D'Andrea MR, Sarmiento R, Salerno F, Gasparini G. Integrated therapy of kidney cancer. *Ann Oncol*. 2007;18 Suppl 6:vi141–8. doi:10.1093/annonc/mdm244
4. Nasrallah D, Abdelhamid A, Tluli O, Al-Haneedi Y, Dakik H, Eid AH. Angiotensin receptor blocker-neprilysin inhibitor for heart failure with reduced ejection fraction. *Pharmacol Res*. 2024;204:107210. doi:10.1016/j.phrs.2024.107210
5. Ksiazek SH, Hu L, Ando S, et al. Renin-angiotensin-aldosterone system: from history to practice of a secular topic. *Int J Mol Sci*. 2024;25:4035. doi:10.3390/ijms25074035

6. Drobni ZD, Michielin O, Quinaglia T, et al. Renin-angiotensin-aldosterone system inhibitors and survival in patients with hypertension treated with immune checkpoint inhibitors. *Eur J Cancer*. 2022;163:108–118. doi:10.1016/j.ejca.2021.12.024
7. Lozinski M, Lumbers ER, Bowden NA, et al. Upregulation of the renin-angiotensin system is associated with patient survival and the tumour microenvironment in glioblastoma. *Cells*. 2024;13:634. doi:10.3390/cells13070634
8. Ekambaram P, Lee JL, Hubel NE, et al. The CARMA3-Bcl10-MALT1 signalosome drives NFkappaB activation and promotes aggressiveness in angiotensin II receptor-positive breast cancer. *Cancer Res*. 2018;78:1225–1240. doi:10.1158/0008-5472.CAN-17-1089
9. Li JH, Wu X, Ni X, et al. Angiotensin receptor blockers retard the progression and fibrosis via inhibiting the viability of (AGTR1+) CAFs in intrahepatic cholangiocarcinoma. *Clin Transl Med*. 2023;13:e1213. doi:10.1002/ctm2.1213
10. Xiong L, Wei Y, Zhou X, et al. AGTR1 inhibits the progression of lung adenocarcinoma. *Cancer Manag Res*. 2021;13:8535–8550. doi:10.2147/CMAR.S335543
11. Zong H, Yin B, Zhou H, Cai D, Ma B, Xiang Y. Loss of angiotensin-converting enzyme 2 promotes growth of gallbladder cancer. *Tumour Biol*. 2015;36:5171–5177. doi:10.1007/s13277-015-3171-2
12. Dong F, Li H, Liu L, et al. ACE2 negatively regulates the Warburg effect and suppresses hepatocellular carcinoma progression via reducing ROS-HIF1alpha activity. *Int J Biol Sci*. 2023;19:2613–2629. doi:10.7150/ijbs.81498
13. Nagappan A, Kim KH, Moon Y. Caveolin-1-ACE2 axis modulates xenobiotic metabolism-linked chemoresistance in ovarian clear cell carcinoma. *Cell Biol Toxicol*. 2023;39:1181–1201. doi:10.1007/s10565-022-09733-1
14. Braun DA, Hou Y, Bakouny Z, et al. Interplay of somatic alterations and immune infiltration modulates response to PD-1 blockade in advanced clear cell renal cell carcinoma. *Nature Med*. 2020;26:909–918. doi:10.1038/s41591-020-0839-y
15. Purdue MP, Rhee J, Moore L, et al. Differences in risk factors for molecular subtypes of clear cell renal cell carcinoma. *Int J Cancer*. 2021;149:1448–1454. doi:10.1002/ijc.33701
16. Yin L, Li W, Xu A, et al. SH3BGRL2 inhibits growth and metastasis in clear cell renal cell carcinoma via activating hippo/TEAD1-Twist1 pathway. *EBioMedicine*. 2020;51:102596. doi:10.1016/j.ebiom.2019.12.005
17. Carey MF, Peterson CL, Smale ST. Chromatin immunoprecipitation (ChIP). *Cold Spring Harb Protoc*. 2009;2009:dbprot5279. doi:10.1101/pdb.prot5279
18. Mei J, Cai Y, Xu R, et al. Angiotensin-converting enzyme 2 identifies immuno-hot tumors suggesting angiotensin-(1–7) as a sensitizer for chemotherapy and immunotherapy in breast cancer. *Biol Procedures Online*. 2022;24. doi:10.1186/s12575-022-00177-9
19. Yin L, Li W, Chen X, et al. HOOK1 inhibits the progression of renal cell carcinoma via TGF-beta and TNFSF13B/VEGF-A axis. *Adv Sci*. 2023;10:e2206955. doi:10.1002/advs.202206955
20. Yin L, Li W, Wang G, et al. NR1B2 suppress kidney renal clear cell carcinoma (KIRC) progression by regulation of LATS 1/2-YAP signaling. *J Exp Clin Cancer Res*. 2019;38:343. doi:10.1186/s13046-019-1344-3
21. Ljungberg B, Bensalah K, Canfield S, et al. EAU guidelines on renal cell carcinoma: 2014 update. *Eur Urol*. 2015;67:913–924. doi:10.1016/j.eururo.2015.01.005
22. Khan Z, Cao DY, Giani JF, et al. Overexpression of the C-domain of angiotensin-converting enzyme reduces melanoma growth by stimulating M1 macrophage polarization. *J Biol Chem*. 2019;294:4368–4380. doi:10.1074/jbc.RA118.006275
23. Danilov SM, Metzger R, Klieser E, Sotlar K, Trakht IN, Garcia JGN. Tissue ACE phenotyping in lung cancer. *PLoS One*. 2019;14:e0226553. doi:10.1371/journal.pone.0226553
24. Jinesh GG, Brohl AS. Classical epithelial-mesenchymal transition (EMT) and alternative cell death process-driven blebbishield metastatic-witch (BMW) pathways to cancer metastasis. *Signal Transduct Target Ther*. 2022;7:296. doi:10.1038/s41392-022-01132-6
25. Bernstein KE, Shen XZ, Gonzalez-Villalobos RA, et al. Different in vivo functions of the two catalytic domains of angiotensin-converting enzyme (ACE). *Curr Opin Pharmacol*. 2011;11:105–111. doi:10.1016/j.coph.2010.11.001
26. Shao M, Wen ZB, Yang HH, et al. Exogenous angiotensin (1-7) directly inhibits epithelial-mesenchymal transformation induced by transforming growth factor-beta1 in alveolar epithelial cells. *Biomed Pharmacother*. 2019;117:109193. doi:10.1016/j.biopha.2019.109193
27. Yong C, Stewart GD, Frezza C. Oncometabolites in renal cancer. *Nat Rev Nephrol*. 2020;16:156–172. doi:10.1038/s41581-019-0210-z
28. Kulkarni PP, Tiwari A, Singh N, et al. Aerobic glycolysis fuels platelet activation: small-molecule modulators of platelet metabolism as anti-thrombotic agents. *Haematologica*. 2019;104:806–818. doi:10.3324/haematol.2018.205724
29. Shi Y, Zhang Q, Bi H, et al. Decoding the multicellular ecosystem of vena caval tumor thrombus in clear cell renal cell carcinoma by single-cell RNA sequencing. *Genome Biol*. 2022;23:87. doi:10.1186/s13059-022-02651-9
30. Psutka SP, Leibovich BC. Management of inferior vena cava tumor thrombus in locally advanced renal cell carcinoma. *Ther Adv Urol*. 2015;7:216–229. doi:10.1177/1756287215576443
31. Xiong W, Zhang B, Yu H, Zhu L, Yi L, Jin X. RRM2 regulates sensitivity to sunitinib and PD-1 blockade in renal cancer by stabilizing ANXA1 and activating the AKT pathway. *Adv Sci*. 2021;8:e2100881. doi:10.1002/advs.202100881
32. Li Y, Shen Z, Jiang X, et al. Mouse mesenchymal stem cell-derived exosomal miR-466f-3p reverses EMT process through inhibiting AKT/GSK3beta pathway via c-MET in radiation-induced lung injury. *J Exp Clin Cancer Res*. 2022;41:128. doi:10.1186/s13046-022-02351-z
33. Cosimo E, Tarafdar A, Moles MW, et al. AKT/mTORC2 inhibition activates FOXO1 function in CLL cells reducing B-cell receptor-mediated survival. *Clin Cancer Res*. 2019;25:1574–1587. doi:10.1158/1078-0432.CCR-18-2036
34. Mossmann D, Park S, Hall MN. mTOR signalling and cellular metabolism are mutual determinants in cancer. *Nat Rev Cancer*. 2018;18:744–757. doi:10.1038/s41568-018-0074-8
35. Murugan AK. mTOR: role in cancer, metastasis and drug resistance. *Semi Cancer Biol*. 2019;59:92–111. doi:10.1016/j.semcancer.2019.07.003
36. Knox JJ, Barrios CH, Kim TM, et al. Final overall survival analysis for the Phase II RECORD-3 study of first-line everolimus followed by sunitinib versus first-line sunitinib followed by everolimus in metastatic RCC. *Ann Oncol*. 2017;28:1339–1345. doi:10.1093/annonc/mdx075
37. Lee C-H, Motzer R, Emamekhoo H, et al. Telaglenastat plus everolimus in advanced renal cell carcinoma: a randomized, double-blinded, placebo-controlled, phase II ENTRATA trial. *Clin Cancer Res*. 2022;28:3248–3255. doi:10.1158/1078-0432.CCR-22-0061
38. Cheng ZY, He TT, Gao XM, Zhao Y, Wang J. ZBTB transcription factors: key regulators of the development, differentiation and effector function of T cells. *Front Immunol*. 2021;12:713294. doi:10.3389/fimmu.2021.713294
39. Zhang Z, Wu L, Li J, et al. Identification of ZBTB9 as a potential therapeutic target against dysregulation of tumor cells proliferation and a novel biomarker in liver Hepatocellular carcinoma. *J Transl Med*. 2022;20:602. doi:10.1186/s12967-022-03790-0

40. Xu L, Chen Y, Dutra-Clarke M, et al. BCL6 promotes glioma and serves as a therapeutic target. *Proc Natl Acad Sci U S A*. 2017;114:3981–3986. doi:10.1073/pnas.1609758114
41. Geng R, Zheng Y, Zhou D, Li Q, Li R, Guo X. ZBTB7A, a potential biomarker for prognosis and immune infiltrates, inhibits progression of endometrial cancer based on bioinformatics analysis and experiments. *Cancer Cell Int*. 2020;20:542. doi:10.1186/s12935-020-01600-5

Biologics: Targets and Therapy Dovepress

Publish your work in this journal

Biologics: Targets and Therapy is an international, peer-reviewed journal focusing on the patho-physiological rationale for and clinical application of Biologic agents in the management of autoimmune diseases, cancers or other pathologies where a molecular target can be identified. This journal is indexed on PubMed Central, CAS, EMBase, Scopus and the Elsevier Bibliographic databases. The manuscript management system is completely online and includes a very quick and fair peer-review system, which is all easy to use. Visit http://www.dovepress.com/testimonials.php to read real quotes from published authors.

Submit your manuscript here: https://www.dovepress.com/biologics-targets-and-therapy-journal